

Molecular Level Studies of Polymer Behaviors at the Water Interface Using Sum Frequency Generation Vibrational Spectroscopy

Jeanne M. Hankett, Yuwei Liu, Xiaoxian Zhang, Chi Zhang, Zhan Chen

Department of Chemistry, University of Michigan, Ann Arbor, Michigan 48109

Correspondence to: Z. Chen (E-mail: zhanc@umich.edu)

Received 15 October 2012; revised 5 November 2012; accepted 5 November 2012; published online 18 December 2012

DOI: 10.1002/polb.23221

ABSTRACT: Industrial plastics, biomedical polymers and numerous other polymeric systems are contacted with water for everyday functions and after disposal. Probing the interfacial molecular interactions between widely used polymers and water yields valuable information that can be extrapolated to macroscopic polymer/water interfacial behaviors so scientists can better understand polymer bio-compatibility, hygroscopic tendencies and improve upon beneficial polymer behavior in water. There is an ongoing concerted effort to elucidate the molecular level behaviors of polymers in water by using sum frequency generation vibrational spectroscopy (SFG). SFG stands out for its utility in probing buried interfaces in situ and in real time without disrupting interfacial chemistry. Included

in this review are SFG water interfacial studies performed on poly(methacrylate) and (acrylate)s, poly(dimethyl siloxane)s, poly(ethylene glycol)s, poly(electrolyte)s and other polymer types. The driving forces behind common water/polymer interfacial molecular features will be discussed as well as unique molecular reorientation phenomena and resulting macroscopic behaviors from microscopic polymer rearrangement. © 2012 Wiley Periodicals, Inc. *J. Polym. Sci., Part B: Polym. Phys.* **2013**, *51*, 311–328

KEYWORDS: polymer surfaces and interfaces; sum frequency generation; molecular orientation; vibrational spectroscopy; interfacial structures; water; biomaterials

INTRODUCTION Polymers are used in almost all aspects of modern life. They can be found in applications ranging from medicinal technologies to domestic goods and are found naturally in numerous biosystems. In many situations, these polymer surfaces are contacted with water, aqueous salt solutions, or water vapor. The polymer/water interface has come under great scrutiny over past years as researchers have strived to maximize favorable surface interactions of polymeric materials with water.^{1–12} Take for instance polymer-based medical devices, which may be immersed in complex bio-based buffer systems. These devices are composed of polymers with distinctive traits supportive of hydrophilicity and biocompatibility within the systems. Such polymers have radically altered medicinal testing and therapies to grant us a plethora of modern health service comforts including tubing, prosthetics, probes, and scaffolds. The technological advances for medicinal-use polymers continue to expand. However, to synthesize better, more biocompatible and safe biodegradable polymer systems one must first know what behavioral aspects make the current biopolymers useful.

As it turns out, many favorable macroscopic surface properties of polymers, such as hydrophilicity and biocompatibility, can be correlated to microscopic interactions between polymer surface functional groups and interactions between the

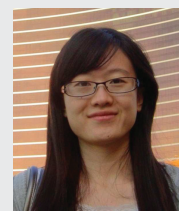
polymer and molecules in the surrounding aqueous environment.^{13–15} This brings up questions such as: what are polymers' microscopic surface behaviors in water? Why and how do they occur? Scientists hope to understand polymer/water interaction by directly probing the molecular level behaviors of polymers that occur at the water/polymer interface. This ultimately means they must understand how surface chemical groups on polymer chains interact with aqueous systems and how this behavior differs from arid chains. The surface chemical groups of such medical-use polymers like poly(methyl methacrylate) (PMMA) may rotate, change orientation, and (dis)order in water and buffers according to their hydrophilicity and chemical makeup.

There are many other categories of polymers where an understanding of the microscopic polymer/water interface is desired. Polymers used for marine antibiofouling purposes sustain especial local molecular interactions with biomatter in water.^{16–18} Scientists have studied the functional groups on marine antibiofouling polymers to understand mechanistic adhesion changes and water's role in removing organisms from man-made surfaces. To improve such antibiofouling systems, molecular level research on polymer functional group orientation changes in aqueous environment has been performed as well.^{19–21} In addition to biofouling, a particular section of recent biopolymer research focuses on polyelectrolytic

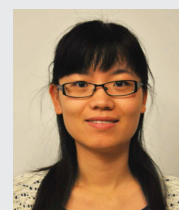
Jeanne M. Hankett is a Ph.D. candidate at the University of Michigan Ann Arbor, pursuing a degree in Analytical Chemistry. She earned her B.S. degree in Chemistry at the University of Illinois at Urbana-Champaign in 2010. She is currently working for Dr. Zhan Chen, where her thesis work focuses on investigating the molecular behavior, orientation, and degradation of phthalates used as plasticizers for PVC at a variety of environmental interfaces.



Yuwei Liu is currently pursuing her Ph.D. in Chemistry under the supervision of Dr. Zhan Chen at the University of Michigan. In the year of 2009, she received her B.S. in Materials Chemistry from Nankai University in China. Her current research interests include mechanisms of antifouling polymeric materials and surface immobilization of peptides and proteins onto solid materials.



Xiaoxian Zhang received her B.S. degree in Material Physics from University of Science and Technology Beijing in 2006 and earned her Ph.D. degree in Physical Electronics from Peking University in 2011. Her current research includes the studies of molecular structures of polymers and low-dielectric materials using nonlinear vibrational spectroscopies. Dr. Zhang is currently a Research Fellow in the group of Professor Zhan Chen at the University of Michigan, Ann Arbor.



Chi Zhang is currently a Ph.D. candidate in Chemistry at the University of Michigan, advised by Prof. Zhan Chen. He earned his B.S. and M.S. in Optoelectronics at Tianjin University in 2006 and 2009. His work now focuses on molecular level understanding of interfaces involving polymers, and developing new nonlinear spectroscopic and microscopic techniques for material and biological study.



Zhan Chen received his B.S. degree from Peking University, M.S. degree from Institute of Physics, Chinese Academy of Sciences and Ph.D. degree from University of California at Berkeley under the guidance of Prof. Herbert Strauss. He then worked as a postdoctoral fellow in Prof. Gabor Somorjai's group at Berkeley. Currently he is a professor of Chemistry at the University of Michigan. His research is to understand molecular structures of polymers and biological molecules at interfaces.



systems, where the interactions between water, charged polymers, and surfactants have been studied. The folding mechanisms of polymers between water and oil interfaces are extremely important in a number of biological systems. Understanding how amphiphilic polymers behave and interact in such hydrophobic/hydrophilic interfaces at a basic level is a key to understanding more complicated biological phenomena like protein folding.²²⁻²⁴

Even more polymers are used in industry as plastics, which may come into contact with different aqueous solutions often during their usable lifetime. The interaction of molecular functional groups in these polymeric materials may drasti-

cally differ according to environmental changes such as humidity levels, changes in pH, and the introduction of other organic materials, all of course depending upon the composition of the polymer chains themselves. As of the last 20 years or so, many questions concerning the polymer swelling and molecular level changes from water contact have remained a mystery. Research in this field has allowed us to understand what aqueous environments aid in the utility of plastics and everyday polymers, and which polymers undergo irreversible molecular changes from water contact.²⁵⁻²⁷

What follows is a concise review on an array of polymers and the studied interactions of these molecules with aqueous

environments. The types of polymers considered include poly(methyl acrylate)s (PMA)s, poly(acrylate)s (PA)s, poly(dimethyl siloxane)s (PDMS)s, poly(ethylene glycol)s (PEG)s, poly(electrolyte)s, poly(urethane) (PU), and poly(styrene) (PS), among others. Owing to the importance of molecular interactions at polymer surfaces, this article focuses solely on the polymer interface rather than bulk materials.

It is difficult to selectively probe the molecular structure of a polymer/water interface *in situ* using traditional analytical techniques. Spectroscopic techniques such as attenuated total reflection Fourier transform infrared spectroscopy (ATR-FTIR) are useful in obtaining data for the top hundreds of nanometers of a polymer sample but cannot selectively probe the monolayer structure at a polymer/water interface.^{28,29} Surface-enhanced Raman spectroscopy is capable of providing highly sensitive surface information of monolayer materials but a specially prepared metal surface is required.^{30–32} In addition, X-ray photoelectron spectroscopy (XPS) is a powerful technique used to obtain chemical bonding information on polymer surfaces and freeze-dry XPS can be used to study atomic level changes due to water exposure. However, both XPS techniques require ultra-high vacuum.^{33–35} Scanning electron microscopy and transmission electron microscopy provide a great deal of insight into polymer surface restructuring from water contact but require vacuum as well.^{36,37} In addition, none of the aforementioned techniques can provide molecular orientation information at interfaces *in situ*. One very powerful analytical technique that may be used to probe polymeric molecules at both surfaces and buried interfaces is near edge X-ray adsorption fine structure (NEXAFS). NEXAFS is capable of giving chemical atomic-level information for less than a monolayer and can even provide information on interatomic distances and molecular orientation. However, this technique requires intense tunable X-rays and for this reason must be performed at synchrotrons.^{38–40}

Arguably, one of the most influential analytical techniques in the polymer/water interface research field is the relatively new spectroscopic tool, sum frequency generation (SFG) vibrational spectroscopy. This technique allows researchers to study molecular vibrations in real time and *in situ* only where centrosymmetry is broken and therefore solely focuses on the water/polymer structured interface, unlike other techniques.^{6,41,42} The unique properties of SFG allow researchers to probe buried interfaces without physically disturbing or pulling apart the polymer from water. The SFG studies presented in this review demonstrate not only the power of this particular technique but the diverse and fascinating interfacial behaviors that polymers undertake in the presence of water.

BASIC SFG THEORY

SFG has been applied to study a variety of polymer interfaces including buried metal/polymer, silica/polymer, polymer/polymer, oil/polymer, and water/polymer as well as air/polymer interfaces.^{6,7,10,25,26,43–56} An SFG process can be considered as a combination of both IR adsorption and

anti-Stokes Raman scattering processes. A visible beam and tunable frequency IR beam must overlap both spatially and temporally on an interface of choice. The resulting sum frequency signal intensity is dominated by the second-order nonlinear susceptibility tensor $\chi^{(2)}$ of the sample.⁴⁹ $\chi^{(2)}$ is a polar tensor which undergoes a sign change after the inversion operation such that $\chi^{(2)}(-r) = -\chi^{(2)}(r)$. For materials with inversion symmetry, nothing will be changed after the inversion operation: $\chi^{(2)}(-r) = \chi^{(2)}(r)$. Most bulk materials contain molecules oriented in an isotropic fashion and therefore can be considered centrosymmetric. The only possible solution for the above relations in such cases is $\chi^{(2)}(r) = 0$ and then SFG signal cannot be generated. However, centrosymmetry is broken at surfaces and interfaces, and $\chi^{(2)}(-r) = \chi^{(2)}(r)$ no longer holds so an SFG signal can be generated. The equation for the intensity of the signal is given below:

$$I(\omega) = \frac{8\pi^3 \omega^2 \sec^2 \beta}{c^3 n(\omega) n(\omega_1) n(\omega_2)} \left| \chi_{\text{eff}}^{(2)} \right|^2 I_1(\omega_1) I_2(\omega_2), \quad (1)$$

where $n(\omega)$ is the refractive index of a medium at frequency ω , β is the reflection angle of the sum frequency field, $I_1(\omega_1)$ and $I_2(\omega_2)$ are the intensities of the two input fields, respectively, and $\chi_{\text{eff}}^{(2)}$ is the effective second-order nonlinear susceptibility tensor of the surface. The magnitude of $\chi_{\text{eff}}^{(2)}$ is proportional to the number of vibrationally resonant surface functional groups. With a visible and an IR beam inputs applied to a sample, if the IR frequency ω_2 is near vibrational resonances, $\chi_{\text{eff}}^{(2)}$ can be expressed as a sum of Lorentzian functions:

$$\chi_{\text{eff}}^{(2)} = \chi_{\text{nr}}^{(2)} + \sum_q \frac{A_q}{\omega_2 - \omega_q + i\Gamma_q} \quad (2)$$

where $\chi_{\text{nr}}^{(2)}$ arises from nonresonant background contributions, A_q , ω_q , and Γ_q are the strength, resonant frequency, and damping coefficient of the q th vibrational mode, respectively. The values of these parameters may be obtained by fitting SFG spectra. The Lorentzian function is typically used to fit SFG spectra because the expression for second-order susceptibility $\chi^{(2)}$ as derived from density matrix theory has the functional form of a Lorentzian.^{6,57} Further details of SFG theory can be found in other publications.^{44,45,57–60}

SFG can be used to determine the molecular structure of the surface or interface involving polymer materials. It can probe the presence, coverage, and orientation (in relation to the surface normal) of functional groups in polymers and other organic compounds. The presence of various functional groups at interfaces can be deduced from various peak centers in the SFG spectra. The interfacial coverage can be inferred from the SFG signal intensity (if certain information is known). In addition, the orientation angles of these chemical groups can be calculated by comparing the components of $\chi^{(2)}$ in different polarization combinations. A typical SFG polarization combination involves polarizing the signal and the visible beams perpendicular to the plane of incidence (s), and the IR beam parallel to the plane of incidence (p),

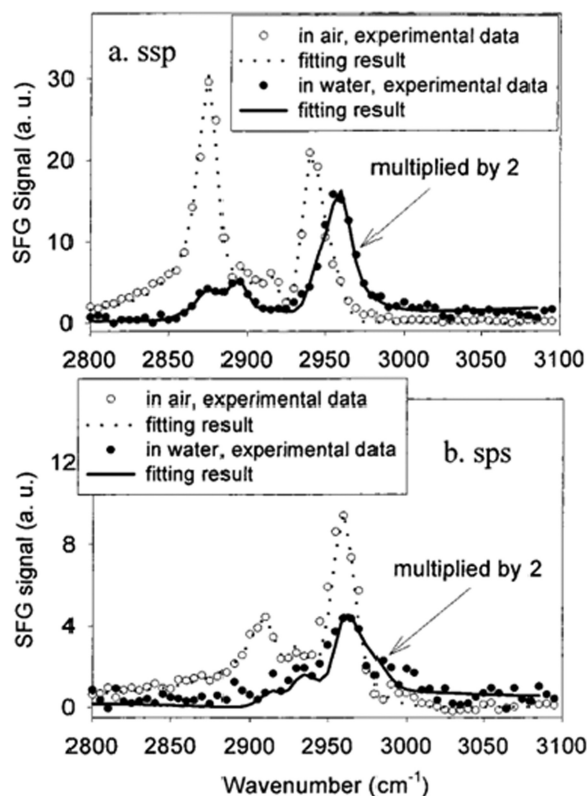


FIGURE 1 SFG spectra of PBMA in air and water for (a) ssp and (b) sps polarization combinations. Reproduced from Ref. 7, with permission from the American Chemical Society.

for an ssp signal combination. Other commonly used combinations include sps and ppp. The components of $\chi^{(2)}$ in these polarization combinations are measured by fitting SFG spectra and can be correlated to the molecular hyperpolarizabilities to determine the molecular orientation. For example, by combining the measured ratio of the $\chi^{(2)}$ components and the relation between these ratios and molecular orientations, the possible molecular orientations of functional groups may be obtained. This information is often applied to CH_3 , CH_2 , and $\text{C}=\text{O}$ groups for polymers.^{61–63}

POLY(METHACRYLATE)/WATER INTERFACE AND POLY(ACRYLATE)/WATER INTERFACE STUDIES

PMAs with Different Side-Chain Lengths Probed in the C–H Spectral Region

Early SFG polymer/water studies used simple polymer systems like poly(methyl acrylate)s to demonstrate the ability of polymer functional groups to order differently under varying chemical environments due to drives toward lowering the system's free energy.^{45,55} An example of such research was reported in 2002 on poly(*n*-butyl methacrylate) (PBMA)⁷ by Chen et al. Here, the average orientation and orientation distribution of methyl groups on the ester side chains of PBMA (Fig. 1) were determined to be different in air and water respectively, using ssp and sps polarized SFG spectral measurements.

In air, the ssp spectrum was dominated by a peak at 2875 cm^{-1} assigned to the symmetric (s) stretch of the methyl group and the 2940 cm^{-1} Fermi resonance peak. In water, however, the asymmetric (as) methyl 2960 cm^{-1} peak dominated instead of the symmetric stretch. Comparatively, this peak dominated both water and air sps spectra and an asymmetric methylene peak at 2915 cm^{-1} was present as well. By deducing the $\chi^{(2)}$ components of the methyl groups from the spectra in Figure 1, it was found that the distribution of CH_3 angles was narrower in water than in air, suggesting there was a higher degree of surface ordering of PBMA groups in aqueous environments (Fig. 2).

In water, the hydrophobic side-chain methyl groups were also measured to tilt more toward the polymer surface whereas in air they stood up. This particular PBMA article gave insight into the interfacial behaviors of biocompatible polymers in water settings.⁷ The drive for hydrophobic components to shift away from the water bulk is a concept that has been found to be applicable for many polymer systems.

In 2001, Chen et al. demonstrated that the behavioral changes of poly(methacrylate)s (PMA)s in water were dependent on the length of the functional groups on PMA side chains as well as hydrophobicity.⁵⁴ PMMA, PBMA, and poly(*n*-octyl methacrylate) (POMA) films were probed in air and in water using SFG. This study demonstrated that the glass transition temperature (T_g) of the polymeric molecules, or the mobility of the polymer backbones, is directly related to the types of molecular movements when polymer chains are in contact with water. PMMA demonstrated no surface

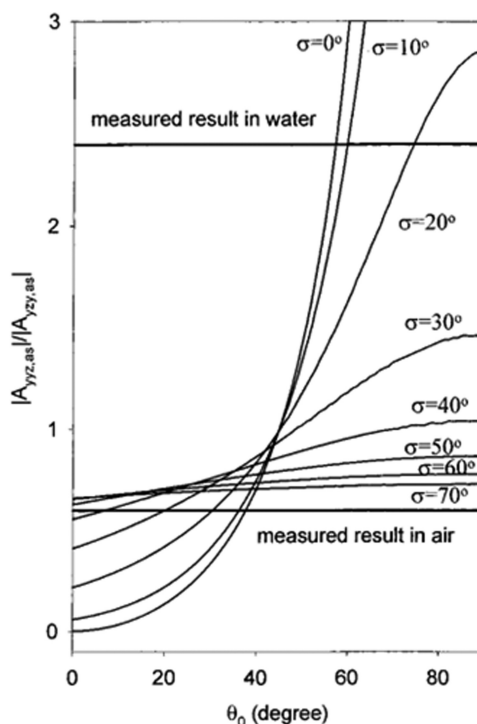


FIGURE 2 $\chi^{(2)}$ component ratio of methyl group as a function of orientation angle θ and angle distribution σ . Reproduced from Ref. 7, with permission from the American Chemical Society.

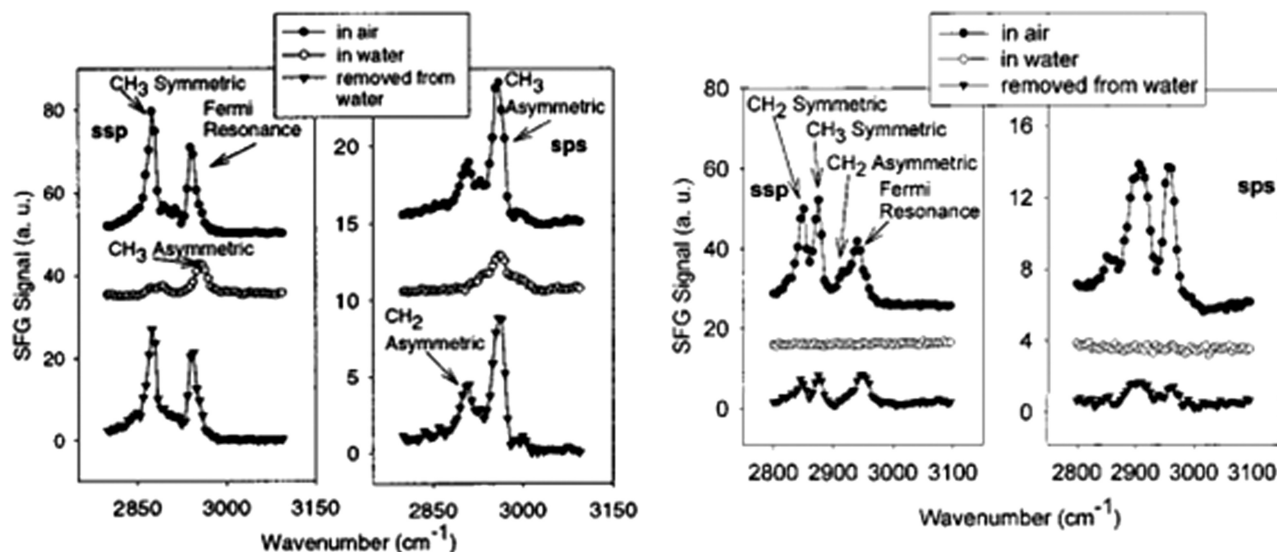


FIGURE 3 SFG spectra of PBMA before, during, and after contacting water (left image). SFG spectra of POMA before, during, and after contacting water (right image). Reproduced from Ref. 54, with permission from the American Chemical Society.

restructuring in water for surface dominating ester methyl groups, due to the PMMA rigid structure (high T_g) and the hydrophilicity of the ester methyl group (compared to the regular methyl group). PBMA underwent surface CH_3 reorientation in water. When the PBMA polymer was removed from water and dried, the original SFG air/polymer spectra returned, suggesting reversible restructuring due to water contact. However, when the POMA was contacted with water, SFG signals disappeared. On drying, the SFG spectra did not return to the normal air interface signals. These trends can be observed in Figure 3.

The data suggested that the POMA surface change after contact with water was not reversible due to backbone changes in water. The longer chain functionalities on the backbone allowed the polymer to be more mobile than PMMA and PBMA and therefore have a comparably lower T_g . On the other hand, the more rigid structures of PMMA and PBMA did not undergo such backbone changes in water and the surface orientations of the methyl groups either did not change or changed reversibly.⁵⁴

Similarly, in 2006 a more detailed study by Chen's group on a wide variety of poly(*n*-alkyl methacrylate)s showed the orientation of the methyl side groups on PMA ester chains varied in accordance with the side-chain lengths.⁵³ In this research, not only were surface restructuring differences of PMMA, PBMA, and POMA in water observed, but also poly(ethyl methacrylate) (PEMA), poly(propyl methacrylate), poly(hexyl methacrylate), poly(lauryl methacrylate), and poly(octadecyl methacrylate) (PODMA). The relationship between reversibility of water-induced structural changes to glass transition temperature was further extended to the listed polymers, ultimately reinforcing molecular level reasoning behind the restructuring of the PMAs to depend on the length of the side chains. For cases where side chains

were short, little surface restructuring due to water contact occurred excluding a change in surface methyl group orientation. At intermediate side-chain length, like that of POMA, the increased volume of the system allowed for the PMA to gain backbone flexibility. On exposure to water the polymer chains likely reoriented greatly in an irreversible manner. However, some side chains were long enough to increase the rigidity of the PMA backbone, as was the case with PODMA, and once again any spectral changes observed due to water contact were reversible on exposure to air.⁵³

SFG spectral interpretation is not always straight forward.^{61,64} The above SFG studies used polymer thin films prepared on solid substrates. When functional polymeric groups order at both an air or water interface and at the interface of the substrate that the polymer is applied to, these signals may interfere with one another and complicate spectra. This ordering is often not an issue for spectral interpretation. Due to both the degree of functional group ordering and refractive indices of interfacial materials, the intensity of SFG signals at the air and water interface are often

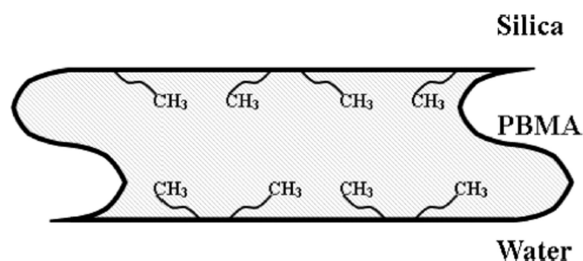


FIGURE 4 Schematic of absolute orientation of side chain methyl groups at the silica/PBMA and PBMA/water interfaces. Reproduced from Ref. 51, with permission from the American Chemical Society.

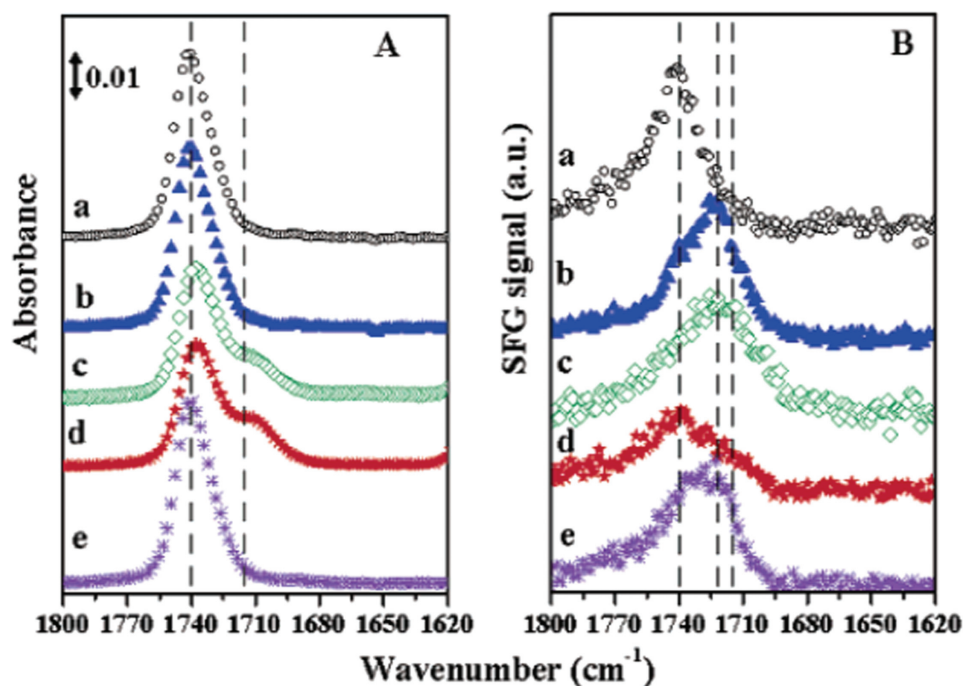


FIGURE 5 IR (left) and SFG (right) spectra of PMEA film in the C=O stretching region (a) before and after immersion in (b) water for 10 s and (c) bisphenol A solution for 10 min (d) bisphenol A in hexane-CHCl₃ for 2 min and (e) after being rinsed by ethanol after (d). Reproduced from Ref. 66, with permission from the American Chemical Society.

more intense than signals at the buried substrate interface. In such cases, the air or water signals completely overwhelm the buried interface signals such that they can be ignored. However, when a polymer film with a certain thickness is chosen, and when the polymer signals at the polymer/water interface are small, the signals from the buried substrate interface cannot be ignored.

The Chen laboratory studied a case of PBMA film sandwiched between a substrate and water where this statement holds true.⁵¹ The side-chain methyl groups of PBMA obtained opposite vibrational phases at the buried substrate (silica) interface and at the water interface. The researchers used the sign (positive and negative) of vibrational phases to assign PBMA CH₃ orientations. Because the two interfaces had opposite signs for the CH₃ vibrational mode, it was believed that both sets of interfacial CH₃ groups pointed toward PBMA bulk (Fig. 4).

While this article focused more on SFG theory and spectral interpretation than the behavior of PBMA functional groups in water, it did demonstrate the observation of PBMA's methyl side chains orienting at two interfaces simultaneously. It also demonstrated the physical importance of peak phase in SFG spectra.⁵¹

PMA/Aqueous Solution Interface as a Function of pH Probed in the C-H Spectral Region

The Ye group recently published a study on the degree of water left adsorbed to the chains of a PMA polyelectrolyte after the polymer was dried.⁶⁵ The topic of polyelectrolyte behavior in water will be explored further in a later section.

For this particular research, the focus was on changes in poly[2(dimethylamino)ethyl methacrylate] (PDMAEMA) water adsorption due to pH changes. This polymer functions as a weak polyelectrolyte in charged solutions. SFG signals were obtained for water vibrations after the polymer was removed from water. It was observed that there was a linear relationship with H₂O signal intensity and polymer weight (i.e., H₂O intensity was directly related to the amount of H₂O molecules still attached to the polymer). The SFG H₂O signal after removal from water at lower pH values (i.e., 4.2), was more intense than at higher pH values (i.e., 7.1). This was believed to have occurred because between pH values of 4.2 and 7.1, the polymer became less and less charged.⁶⁵ As the polymer was removed from buffer and dried, charged sections of the polymer held attraction to water molecules better than uncharged sections. Therefore, at lower pH values, it would be expected that the polymer would hold more water molecules and weigh more.

pH cannot only affect hydrogen bonding on polymers but conformation of alkyl groups as well. In a 2012 study by Wu et al., poly[2-(dimethylamino)ethyl methacrylate] (PDEM) was found to behave differently in buffer solutions according to how protonated the polymer was. The polymer was applied over water with controlled pH using hydrochloric acid and sodium hydroxide so that it was sandwiched between air and a buffer. At pH 4, the amine groups on PDEM were fully charged. This allowed the polymer to integrate fully with water under the film and the chains were drawn into the water phase, giving no SFG signal. At a pH of 7, the polymer was partially charged and some of the alkyl

groups stood up in the air, giving signal for methyl and methylene groups. At pH 10, the amine groups were uncharged, allowing these groups to protrude further into the air, at a more perpendicular angle to the surface normal than previously. As a result, the methylene and methyl peaks associated with the amine groups were stronger in the SFG spectra.⁵²

PMAs and PAs Probed in the C=O Spectral Region

In addition to studying methyl groups on PMAs, SFG has also been utilized to observe hydrogen bonding in acrylate polymer systems. In 2004, Li et al. focused on hydrogen bonding with poly(2-methoxyethyl acrylate) or PMEA in water to better understand the role of polymer hydrogen bonding in biocompatibility.⁶⁶ This behavior can be extended to a system where hydrogen bonding between functional groups on polymers and water at polymer/water interface occurs. When PMEA was contacted with water, after only 10 s an 18 cm⁻¹ red shift appeared for a band at 1740 cm⁻¹, assigned to the PMEA C=O groups, which suggested the C=O groups underwent hydrogen bonding with water molecules. In contrast such shift was not seen in IR spectra, and therefore the PMEA bulk did not experience such hydrogen bonding.⁶⁶ This trend can be observed in Figure 5.

The water-induced C=O bond changes of polyacrylates were also studied in PEMA compared to poly(ethyl acrylate) (PEA) in 2005 by Chen et al.⁶⁷ Both PEMA and PEA C=O peaks observed a red shift on immersion in water of about 10–20 cm⁻¹, due to hydrogen bonding between the polymer and water. PEMA also had stronger signals compared to PEA, which suggested these C=O bonds were more highly ordered than those in PEA. Finally, the stronger decrease in signal intensity for PEA compared to PEMA suggested there was a loss of order within the backbone. This study demonstrated there are large differences in polymer behaviors in water even with very similar surface structures in air.

SFG has also been applied to investigate the surface C=O stretching signals of PMMA, PBMA, POMA, and PODMA in air and in water.⁶⁸ The Chen laboratory found that the C=O orientations on the different PMA surfaces in air are quite different, but they are similar in water after the formation of hydrogen bonds.

In this section, we have seen hydrophobic groups on PMAs like CH₃ order differently in air than water, lying down closer to the polymer surface more in water. The degree of surface reordering and reorientation of these groups in water depends on the length of functional groups on PMA chains, and on the rigidity of the backbone. We have also observed that environmental pH changes both the degree of hydrogen bonding between the polymer and water and the conformation of the polymer's side-chain alkyl groups. In addition to obtaining vibrational information about hydrophobic PMA groups and water, SFG has been used to observe interfacial hydrogen bond formation. We have seen that PMAs' and PAs' C=O groups may undergo different degrees of hydrogen bonding with water molecules at the interface.

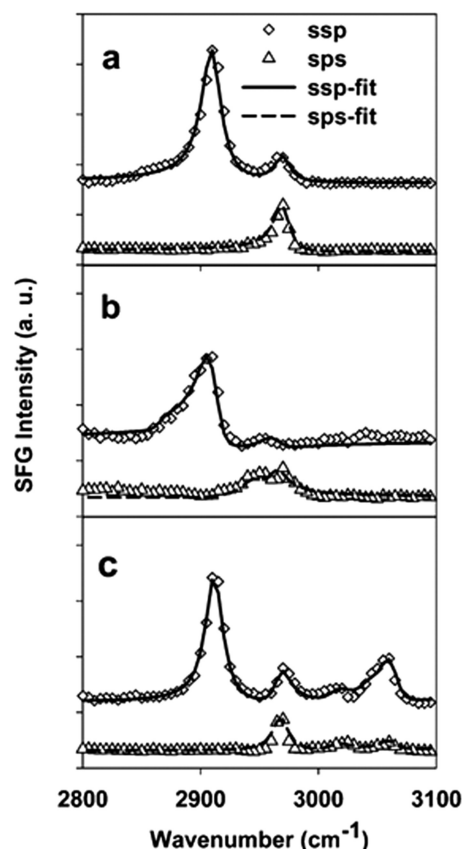


FIGURE 6 Measured and fitted SFG spectra (ssp and sps) from three PDMS surfaces in air (a) TEOS-PDMS, (b) Pt-PDMS, and (c) PDMS-co-PS. Reproduced from Ref. 26, with permission from the American Chemical Society.

POLY(DIMETHYL SILOXANE)/WATER STUDIES

Crosslinked PDMS

Many polymers have beneficial molecular behaviors in aqueous environments that may be enhanced by increasing the complexity of the polymer chains and therefore the polymer network. Such behaviors are observed with poly(dimethyl siloxane)s, which are often applied in both the medical field and for marine biofouling control.^{69,70} An example of the differences in water restructuring behavior between different PDMS materials can be found in Chen's article in 2004.²⁶ Here, the crosslinked polymers tetraethoxysilane cured hydroxyl-terminated PDMS (TEOS-PDMS), platinum cured vinyl-terminated PDMS (Pt-PDMS), and PDMS-co-polystyrene (PDMS-co-PS) copolymer were investigated in both air and water.

In air, the three polymers contained a Si—CH₃(s) stretch at 2910 cm⁻¹ and a CH₃(as) stretch at 2965 cm⁻¹ in the ssp spectra. Additional signal was observed for Pt-PDMS around 2865 cm⁻¹, which was attributed to methylene groups at crosslinking points. For PDMS-co-PS, the dominating air SFG signals were due to methyl groups, suggesting PDMS dominates the surface. After orientation analysis, it was demonstrated that the methyl groups on all three PDMS surfaces

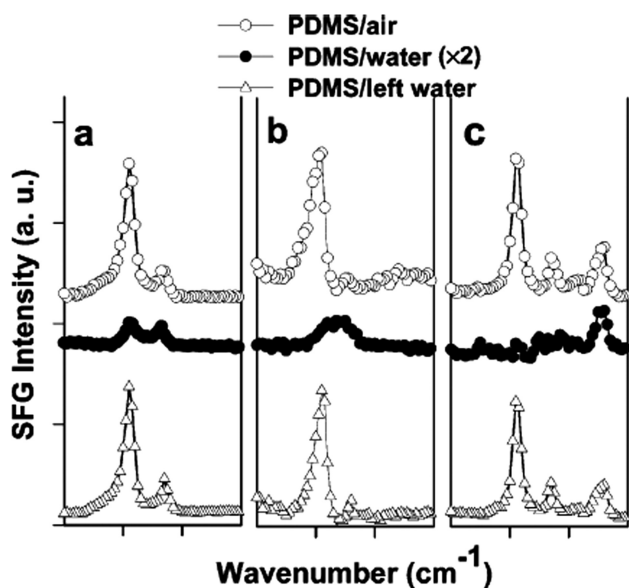


FIGURE 7 Measured and fitting SFG spectra (ssp) collected from three PDMS/water interfaces (a) TEOS-PDMS, (b) Pt-PDMS, and (c) PDMS-co-PS. Reproduced from Ref. 26, with permission from the American Chemical Society.

adopted a similar orientation at the air interface of about 40° to the surface normal, assuming a delta-function angle distribution (Fig. 6).²⁶

Once the PDMS films were contacted to water, the spectra were quite different. In water the TEOS-PDMS and Pt-PDMS spectra had a different CH_3 (as) to CH_3 (s) signal strength ratio, suggesting the methyl groups were tilting further toward the surface. Further calculations demonstrated that there was a narrower distribution of molecular orientation angles in water than in air. The PDMS-co-PS film behaved quite differently in water. Here the signals of methyl groups disappeared and only spectral peaks due to phenyl groups were present. This might have been due to the higher rigidity of the PS backbone compared to the PDMS-while methyl groups in PDMS disordered in water, the phenyl groups remained rigidly in place. After removing the PDMS films from water, SFG air spectra recovered. This suggested that the polymer surface change in water was reversible, and the films were stable in water, likely due to crosslinking (Fig. 7). For reference, the scale in Figure 7 ranges from 2800 to 3100 cm^{-1} (the same range as in Fig. 6).

For comparison, a partially crosslinked PDMS sample was probed before and after water contact. The spectra were not identical. This research demonstrated the benefits of synthesizing more complicated PDMS materials. While the functional groups move in aqueous environments to lower the surface energy, the two cured PDMS and PDMS-co-PS polymers are stable and return to an equilibrium state on drying.²⁶

PDMS Grafted Polymers

PDMS polymers may be grafted to other polymer types to increase the system's biocompatibility.^{71,72} The Somorjai labo-

ratory studied a complicated commercially available polymer called BioSpan-S in 1997, a polyurethane-type polymer that was grafted with PDMS end groups and designed to be biocompatible.⁴⁴ By performing SFG experiments *in situ*, the BioSpan-S/water interfacial changes were tracked over time. Within a period of 51 h, the polymer significantly restructured from the air interface. The methyl group peak of PDMS at 2919 cm^{-1} decreased over time whereas the peaks of the CH_2 BioSpan-S groups increased in intensity. The belief here was the more hydrophilic BioSpan-S polymer backbone effectively pushed PDMS segments toward the polymer bulk so that they were reoriented to minimize contact with water (Fig. 8).

Like many articles listed above, this study demonstrated a drive to minimize free energy between hydrophobic and hydrophilic interactions.⁴⁴

Biological molecules may undergo undesirable interactions with PDMS's methyl groups, hindering the efficiency of the polymer material and causing some medical issues.^{73,74} To address these challenges, the Chen group studied PDMS surfaces grafted with zwitterionic [2-(methacryloyloxyethyl)-dimethyl(3-sulfopropyl)ammonium (ZW) in 2009. For comparison purposes, PDMS surfaces modified with acrylic acid (AA) and cationic dimethylacrylamide (DMAA) as monomers

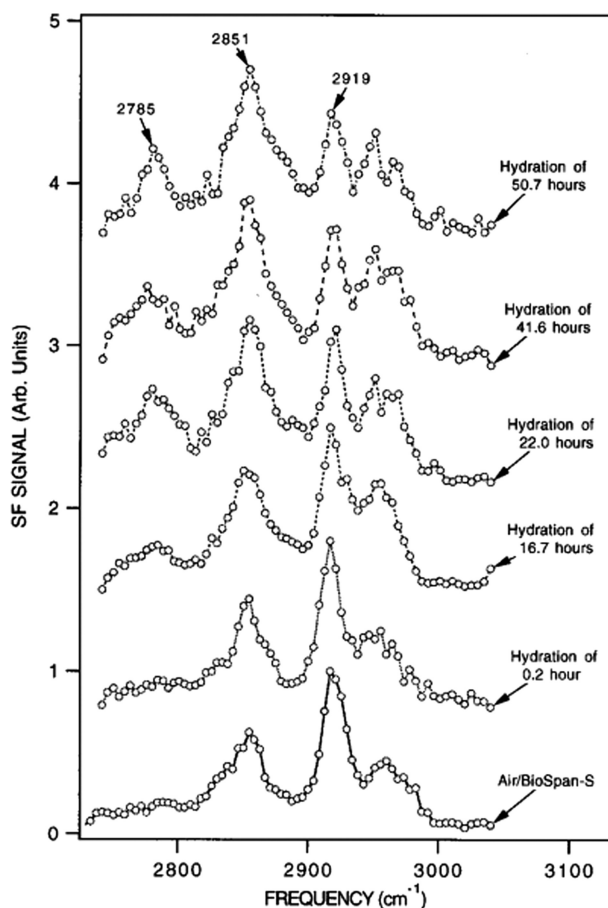


FIGURE 8 Time evolution of SFG (ssp) spectra from the BioSpan-S/water interface. Reproduced from Ref. 44, with permission from the American Chemical Society.

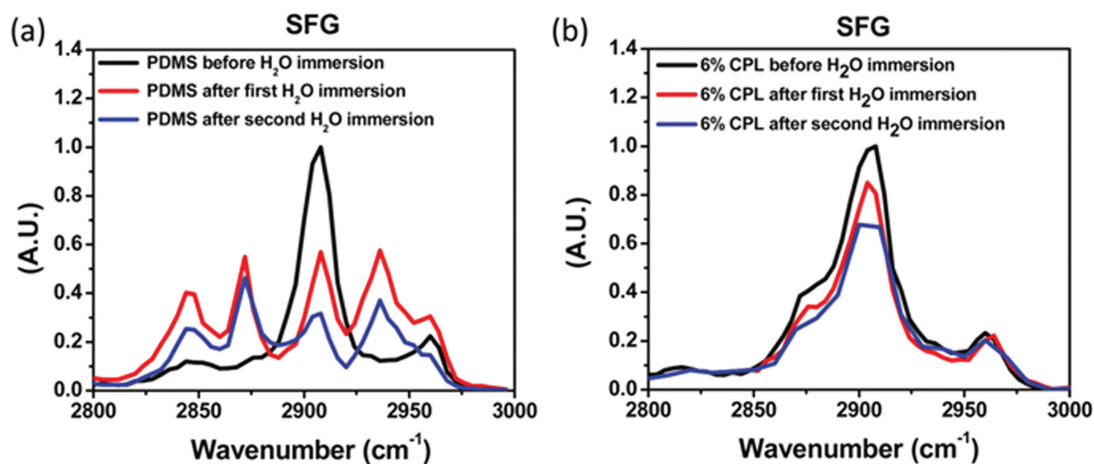


FIGURE 9 SFG spectra of the polymer/air interface before and after immersion in water twice for (a) 2000 g mol^{-1} PDMS and (b) 6% CPL. Reproduced from Ref. 76, with permission from the American Chemical Society.

for polyelectrolytes, designed to increase polymer hydrophilicity were also studied.⁷⁵ SFG spectra of unmodified PDMS, ZW, AA, and DMAA modified PDMS were obtained (all in D_2O). For pure PDMS, the two peaks around 2915 and 2965 cm^{-1} were due to the symmetric and asymmetric CH stretches of the $\text{Si}-\text{CH}_3$ groups, respectively. The ZW and DMAA modified PDMS were dominated by a peak at 2945 cm^{-1} , attributed to Fermi resonance from the polyelectrolyte. The AA spectrum was dominated by a peak at 2930 cm^{-1} likely due to the asymmetric methylene stretch of the polyelectrolytic material. This suggested that in water, the hydro-

philic segments of the PE migrated to the interface, forming a hydrophilic surface, and the PDMS segments went to the bulk, much like the behavior found with BioSpan-S in water.⁷⁵

PDMS and Lubricants

Grafting PDMS to other organic groups is not the only way to increase PDMS's compatibility and structural integrity in water. As shown in this 2011 article by Kim et al., a cationic polymer lubricant (CPL) was added to PDMS, preventing the dewetting of the polymer after successive immersions in water.⁷⁶ Figure 9 shows SFG air/polymer spectra of pure PDMS (right) and PDMS with 6% CPL (left) before and after water immersion, and after a second immersion.

As can be observed with pure PDMS, extra peaks appeared at 2844 , 2876 , and 2936 cm^{-1} after immersion in water, which were attributed to organic contaminants. Such contaminants can appear on polymer/air surfaces if the surface becomes dewetted. In comparison, the SFG spectra of the PDMS with CPL spectra remained similar before and after water immersion. Symmetric and asymmetric methyl stretching were seen at 2908 and 2960 cm^{-1} , respectively. The shoulder peak at 2876 cm^{-1} was attributed to the methyl symmetric stretching from the CPL ammonium cation. These spectra suggested, disregarding reorientation of $\text{Si}-\text{CH}_3$ groups at the CPL air surface, that this film did not dewet and was more stable after removal from water. Therefore, the addition of CPL to PDMS stabilized the hydrophilic properties of the film's surface.⁷⁶

PDMS Chain Folding

The characterization of PDMS materials discussed in previous sections focused on changes in polymer/water interactions because of PDMS chemical modifications. Presented now is a 2008 Yu group study on the chain conformational behavior of PDMS at an air/water interface.⁷⁷ By taking SFG spectra of different PDMS concentrations layered between an air/water interface, the type and direction of chain layering could be hypothesized. Here, Figure 10 can be separated into

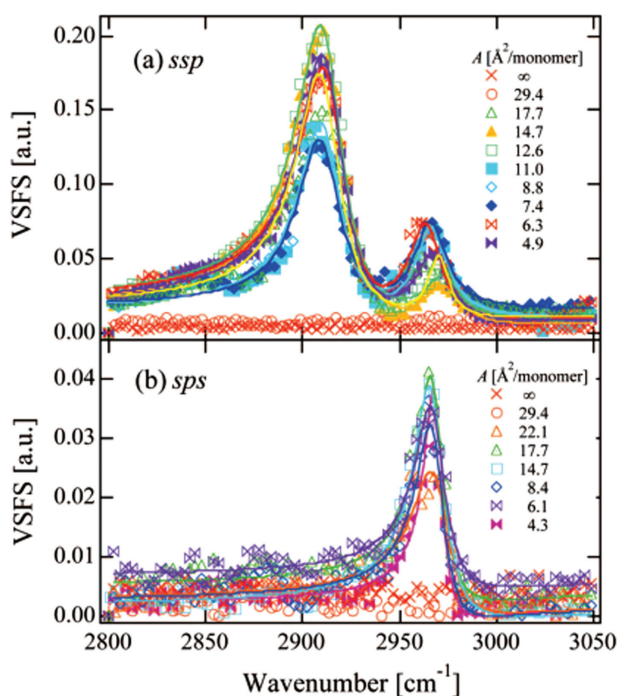


FIGURE 10 SFG spectra of (a) ssp and (b) sps polarization combinations from PDMS monolayer at various surface concentrations. Reproduced from Ref. 77, with permission from the American Chemical Society.

four different distinctive regimes according to the peak shapes.

Using ssp spectra, researchers demonstrated a low concentration of PDMS in which there was no PDMS signal. This is suggestive that on water at low concentrations, PDMS chains were randomly ordered and freely rotating, thus giving no SFG signal. In the second regime, there were two dominant peaks at 2910 and 2965 cm^{-1} (symmetric and asymmetric methyl stretches). For this regime, the laboratory evaluated the $\chi^{(2)}$ contributions of the methyl groups in ssp and sps polarization combinations and concluded the PDMS chains lay on the water/air interface with methyl groups pointing toward the air. One set of methyl groups pointed further away from the surface normal than the other (pointed closer to the polymer surface). There was another clear section of spectra at a different concentration regime, which may have been due to two possible conformations. Either the peak ratios gave horizontally folded layers or formed helices that lay on top of a monolayer of PDMS. Finally, the most concentrated PDMS samples lay on the last regime of spectra where horizontally folded multilayers were likely formed. By determining the average orientation of the methyl groups at different concentrations, a possible picture of how the chains folded and interacted at the air interface was formed.⁷⁷

PDMS Incorporated with Biocides for Marine Anti-biofouling Purposes

Coupling biocides into polymer coatings may be an effective means to prevent biofouling from occurring. PDMS is being developed as a promising fouling-release polymer coating for marine vessels.^{78,79} Incorporating biocides into PDMS may lead to polymer coatings which can have both antifouling and fouling-release characteristics.^{80,81} SFG has been used to characterize the surfaces of PDMS materials with various quaternary ammonium salts (QAS) incorporated into the polymer.^{20,21} In addition, the effects of bulk biocide concentration and the tethered QAS chain length on the surface structure of PDMS incorporated with QAS were investigated. Such surface structures can be well correlated to the anti-fouling activity tested using bacteria.

In a 2008 Chen laboratory study, the differences in surface structure of the polymer/QAS coatings at air and water interfaces were discussed. Tetradecyldimethyl (3-trimethoxysilylpropyl) ammonium chloride (C-14 QAS) was bonded to PDMS. In air, signals at 2857, 2880, and 2940 cm^{-1} attributed to surface segregated QAS groups, were observable along with PDMS vibrational signatures. By comparing SFG signal intensity with FTIR experiments, researchers found the QAS groups segregated to the film surface in air and this content at the surface increased with increased bulk QAS concentration. Comparatively in water, biocide signals were still observable at the interface, although the signal intensity decreased, likely due to the differences in Fresnel coefficients. For the algae *N. incerta*, a bulk-increased concentration of QAS in PDMS was found to directly correlate with a reduction in algal growth.

A 2010 study focused on PDMS modified with various methoxysilane-functional QAS, which contained different alkyl chain lengths attached to the nitrogen atom on QAS and different chain lengths from the nitrogen atom to the silicon atom. SFG results revealed both alkyl chain lengths affected the surface structure of the materials in air. Even so, signals at 2850, 2875, and 2940 cm^{-1} that were attributed to QAS groups demonstrated QAS molecules segregated to all surfaces in air. In water, significant surface restructuring occurred. In certain cases, strong water signals were observed from interfacial water molecular ordering. This was believed to have occurred where the alkyl chains around the QAS did not shield the nitrogen atom, which may have interacted with water. The QAS molecular structure that was found to reduce biofilm retention from a number of alkyl chain ratios contained a shorter alkyl chain between the nitrogen atom and silicon atom coupled with relatively longer alkyl chain on the other side of the nitrogen. This structure was believed to give hydrophobic "shielding" around the nitrogen atom, allowing QAS segregation to the surface and increased interaction with biomatter.^{20,21}

The above section demonstrated that poly(dimethyl siloxane)s follow similar behavioral patterns as poly(methyl acrylate)s, with hydrophobic groups changing orientation and ordering on water contact. We have seen SFG used to observe these basic molecular behaviors and to study behavioral differences once PDMS is altered to improve bulk and surface properties like stability in water, increased hydrophilicity, and biocompatibility. For instance, crosslinked PDMS were found to be more stable in water and PDMS grafted with biofriendly materials contained hydrophobic groups that moved toward the bulk while the hydrophilic groups of the biomaterial moved toward water. In addition, we learned that the addition of surfactant to PDMS could help prevent dewetting of the polymer surface after water immersion. SFG has also been used to study not only small functional groups of PDMS, but the chain folding behaviors at aqueous interfaces, which is unique at the first few chain layers compared to bulk. Finally, we have looked at cases of PDMS modified with QAS compounds studied for marine antibiofouling applications, where the concentration and structure of QAS on PDMS surfaces was well correlated to the degree of the material's antibiofouling capabilities.

POLY(ETHYLENE GLYCOL)/WATER STUDIES

PEGs as Amphiphilic Molecules

We have just observed how PDMS chains can layer differently at an interface. Besides coils and horizontal layers, hydrophobic polymers can take on more complicated conformations in hydrophilic settings such as micelles and polymer brushes.^{82,83} By studying the microscopic ordering of amphiphilic neutral polymers at different interfaces, scientists may better understand the microscopic driving forces behind complicated macroscopic polymer aggregation.⁸⁴⁻⁸⁹ SFG has been applied to study interfacial behavior of PEG, poly(propylene glycol) (PPG), and the copolymer of PEG and PPG.^{88,90-92} The Somorjai group studied the adsorption of

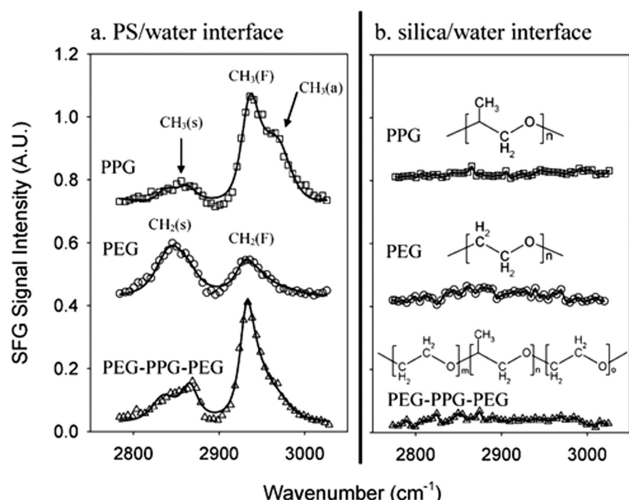


FIGURE 11 SFG spectra for adsorbed PPG (squares), PEG (circles), and PEG-PPG-PEG (triangles) at the (a) PS/water and (b) silica/water interfaces. The solid lines represent spectral fitting results. Reproduced from Ref. 56, with permission from the American Chemical Society.

PEG and PPG, common amphiphilic polymers, in 2003.⁵⁶ Specifically, PEG, PPG, and a triblock PEG-PPG-PEG copolymer were dissolved in deuterium oxide and contacted with either deuterated poly(styrene) on a silica substrate to generate a PS/water interface, or with a clean silica substrate to generate a silica/water interface. The deposited polymers were contacted with water and probed by SFG. The resulting SFG spectra shown in Figure 11 demonstrate that the polymer had a much higher degree of ordering at the PS/water interface compared to the hydrophilic silica/water interface.

The PPG functional groups were assigned as follows: a vibrational signature at 2840 cm^{-1} was due to the $\text{CH}_2(\text{s})$ peak, 2870 cm^{-1} the $\text{CH}_3(\text{s})$, 2940 the CH_3 Fermi resonance and 2970 to $\text{CH}_3(\text{as})$. PEG contained $\text{CH}_2(\text{s})$ stretches at 2865 cm^{-1} and CH_2 Fermi resonance at 2935 cm^{-1} . The hydrophobic sections of PPG and PEG (CH_3 and CH_2 groups) pointed toward the PS at the PS/water interface. However, in the copolymer the functional group behavior was a bit different. The more hydrophobic middle section of this polymer (PPG) contained CH_3 groups that pointed toward the PS interface, but judging by the spectral intensity, the less hydrophobic PEG sections were more disordered. In comparison to the PS/water interface, no peaks were observed from any polymers at the hydrophilic/hydrophilic interface of silica/water. This study suggested that hydrophobic surfaces might be required for amphiphilic polymers to order their hydrophobic components at an interface.⁵⁶

PEGs and Surfactants

The combination of PEGs and anionic surfactants is common in commercial synthesis of polymer biomedical products. The anionic surfactant is believed to interact with the polar water oxygen group so the hydrocarbon groups are more easily hydrated by water. As an example, the Davies group

conducted SFG experiments on PEG mixed with the surfactant sodium dodecyl sulfate (SDS) at the octadecanethiol/aqueous solution interface.⁹³ In Figure 12, SFG spectra of PEG 900 with various concentrations of SDS are plotted.

No SDS adsorption was seen until the concentration was 1:10. With increasing concentrations, the methylene and methyl groups of SDS pointed toward the hydrophobic interface. This study suggested that there is a minimum concentration of SDS required at this particular PEG molecular weight to allow for SDS hydrophobic adsorption at a hydrophobic/hydrophilic interface.⁹³

The Davies group also studied poly(ethylene oxide) (PEO) with different concentrations of SDS and in different environments.⁹⁴ The polymer and surfactant were placed at an octadecane thiol/aqueous interface. Water was then replaced with a 0.1 M NaCl electrolytic solution and SFG spectra at both sets of interfaces were compared. It was found the hydrophobic groups of PEO and SDS interacted similarly in both chemical environments. Any SFG signals observed from the polymer at a hydrophobic interface were eliminated once a minimum concentration of SDS was added required for aggregation. While the exact reasons for SFG signal disappearance remain unclear, it was believed that the original PEO and SDS signals were from CH_2 and CH_3 groups that pointed toward the hydrophobic octadecane thiol interface. Once the SDS concentration was enough a few actions might have occurred. Either PEO desorbed from the interface, the

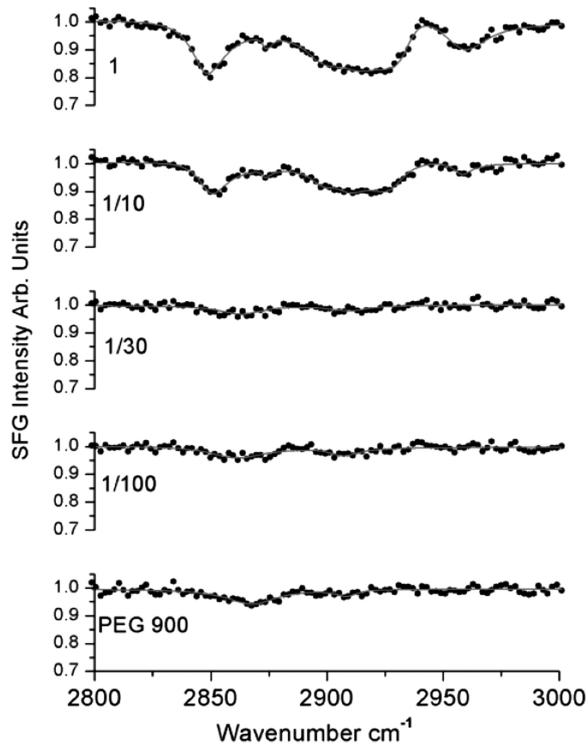


FIGURE 12 Spectra of PEG 900 and PEG 900/SDS adsorbed from binary solution. Reproduced from Ref. 93, with permission from the American Chemical Society.

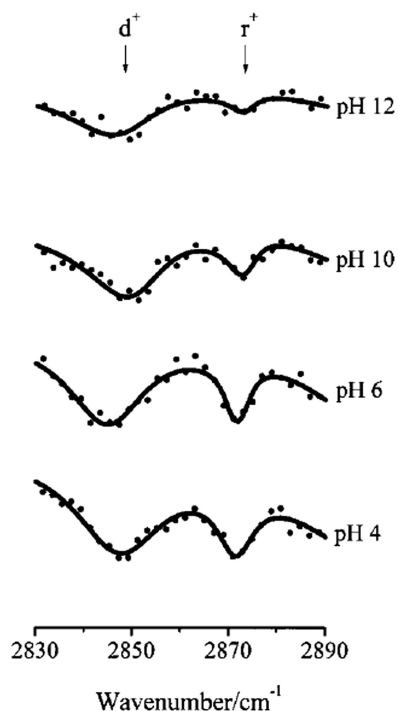


FIGURE 13 SFG spectra (ppp) of SDS adsorbed from 1/100 cmc SDS, 100 ppm PEI, 0.1 M NaCl solution at 18 °C as a function of pH. Reproduced from Ref. 95, with permission from the American Chemical Society.

PEO and SDS interacted with one another to form complexes, or both processes occurred.⁹⁴

Fewer SFG studies have been completed on PEG behavior at the water interface than on PMAs and PDMS, but in this section, we have seen that PEG's hydrophobic functional groups are known to rearrange with different surfactant concentrations, and behave differently at the water interface when PEG is engineered with copolymers.

POLY(ELECTROLYTE)/WATER STUDIES

pH and Poly(electrolyte)s

SFG on poly(electrolyte)s furthers the surfactant polymer studies topic. A surfactant may interact differently with a polymer depending on the temperature or pH of the surrounding environment and that polymer can then behave as a poly(electrolyte). To test this theory, the Davies group studied the molecular interaction between SDS and poly(ethylenimine) (PEI) in solutions of different concentrations and values of pH at the deuterated octadecanethiol/solution interface.⁹⁵ When the pH of the solution containing 100 ppm PEI and 1/100 cmc (critical micelle concentration) SDS was increased, there was a gradual decrease in the SDS CH₃ (s) to CH₂ (s) (2873 and 2845 cm⁻¹, respectively) ratio. Generally speaking if an alkyl chain is ordered at an interface, the CH₂ (s) SFG signal will be small.^{96,97} Comparing the CH₃ to CH₂ signals is a common method of determining changes in alkyl chain ordering. Hence, the decrease in the CH₃/CH₂ in-

tensity ratio for SDS was indicative of a decrease in the degree of SDS alkyl chain order (Fig. 13).

This was likely due to changes in the charge density of the polymer in solution. At lower pH values, the PEI was highly charged and by pH 12, no formal charge was expected to exist. Therefore, at lower pH, the SDS alkyl chain could be ordered by the PEI charges, while at high pH, due to the loss of the charge, the SDS alkyl chain became disordered. Note that the peaks of interest in Figure 13 are pointed downward, or "negatively." We previously stated that the phase of the SFG signal might change in accordance with molecular orientation in PMA/water interface and PA/water interface studies section. This case is no different. The negative peaks in this study were attributed to surfactant molecules that contained hydrocarbon chains oriented toward the polymer surface, whereas positive peaks were assigned to molecules with hydrocarbon chains pointed toward the solution.

The polymer concentration dependent study at a pH of 6.0 was also carried out. At 10 ppm of PEI and higher, the methyl to methylene ratio remained similar. Below 10 ppm not much adsorption was seen. This trend suggested there was a minimum threshold concentration of PEI required to allow for SDS chain order; but above this threshold, additional concentrations of PEI had no effect on the SDS ordering in solution. Similarly, this same group found that PEI ordering was barely affected by SDS concentration in a previous publication.⁹⁵

Oil and water form many ordered interfacial structures in biological systems. The adsorption of polymers at these interfaces is often complicated and difficult to deconvolute with any molecular level technique other than SFG. The adsorption and desorption of poly(acrylic) acid or PAA at an oil/water interface was studied by the Richmond group in 2011.²² It was discovered that PAA behaves quite differently below and above a pH of 4.5 at the water/CCl₄ interface. The adsorption of the polymer was followed in both C=O and CH/OH regions of SFG spectra. The presence of peaks in the CH stretching region suggested polymer order, and therefore adsorption at the interface. Peaks at 2930 and 2850 cm⁻¹ were assigned to the asymmetric and symmetric CH₂ group on PAA, respectively. At low pH values, these peaks dominated spectra but at pHs higher than 4.5, no such peaks were observed. For C=O region spectra, a peak at 1730 cm⁻¹ assigned to the C=O stretch from PAA carboxylic acid groups was present between pH 2 and 4. Above pH 4.5, no C=O stretch was observed. The C-H and C=O spectra suggested the polymer was no longer adsorbing to the oil/water interface at higher pH values.

The OH region was used to observe interfacial ordering of water molecules and confirm or deny this hypothesis. OH stretches at 3700 cm⁻¹ assigned to free water molecules appeared only at pH values above 4.5. This information was used to conclude the CCl₄/water interface contained no polymer chains above pH 4.5. This agrees with a hypothesis of charged polymer states. At increasing pH, the PAA contained higher concentrations of charged carboxyl groups, which

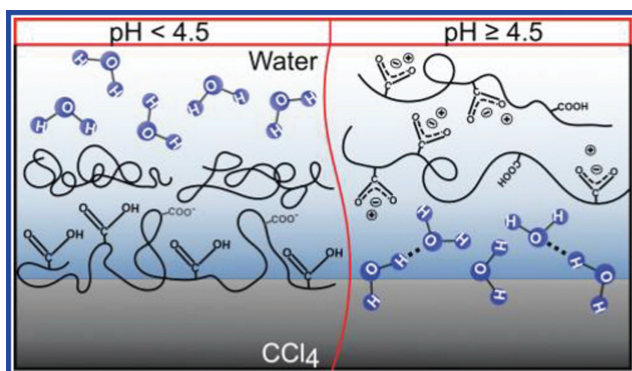


FIGURE 14 Representation of PAA at the CCl_4 /water interface for the two pH regimes. In the low-pH regime (left), polymer adsorbs strongly to the interface with highly oriented carbonyl and CH groups. In the high-pH regime (right), there is a deficit of polymer from the interface, which leaves the water molecules close to their normal neat interfacial structure. Reproduced from Ref. 22, with permission from the American Chemical Society.

underwent repulsive interactions with each other and preferentially interacted with the water phase rather than staying adsorbed at the water/oil interface. As a pictorial reference to the two types of polymer ordering above and below pH 4.5, see Figure 14.²²

The Richmond laboratory continued polyelectrolytic studies at the oil/water interface, expanding research on PAA and studied iso and atactic poly(methyl acrylic acid) (PMAA) in water and CCl_4 .²³ Once again studying pH-dependent polymer ordering, researchers found atactic and isotactic PMAA behave differently at low pH values. In addition, the knowledge of layering behavior of polymers at low pH was expanded. For PAA, adsorption occurred in a two-step process. Tracking the same CH_2 functional groups as the previous article, it was found that a layer of PAA ordered at the water/oil interface in less than 1 min while the remaining polymer chains coiled with increasingly less order the further away they were from the interface. Atactic PMA followed a similar behavioral pattern, but isotactic PMAA was found to be more rigidly structured and as a result, a limited amount of polymer ordered at the interface. All polymers studied only ordered at the interface at lower pH as at this point the polymers were highly uncharged. These studies demonstrated that the tacticity of a polymer greatly changes the ordering behavior of polymers at a Janus interface (Fig. 15).²³

This section reviewed Poly(electrolyte) behaviors at the water interface. Like PEGs, poly(electrolyte)s' functional group behavior can drastically differ depending on the concentration of surfactant nearby and the pH of their surrounding environment. It has been observed that a minimum concentration of poly(electrolyte) is required for ordered surfactant alkyl chains at water. Also, by studying poly(electrolyte)s at the water/oil interface at different pH values, the degree, and type of polymer functional group and chain ordering at a model biological interface can be determined

using SFG. We have seen pH-dependent orientation behavior like poly(electrolyte) ordering at a water/oil interface at lower pHs and have learned that at higher pHs the polymers are more charged and preferentially interact with water rather than oil so they do not order at these interfaces.

MISCELLANEOUS POLYMERS

Polymers with Plasticizers in Water

The introduction of plasticizers to a polymer can radically change the structure of the polymer/water interface. In fact,

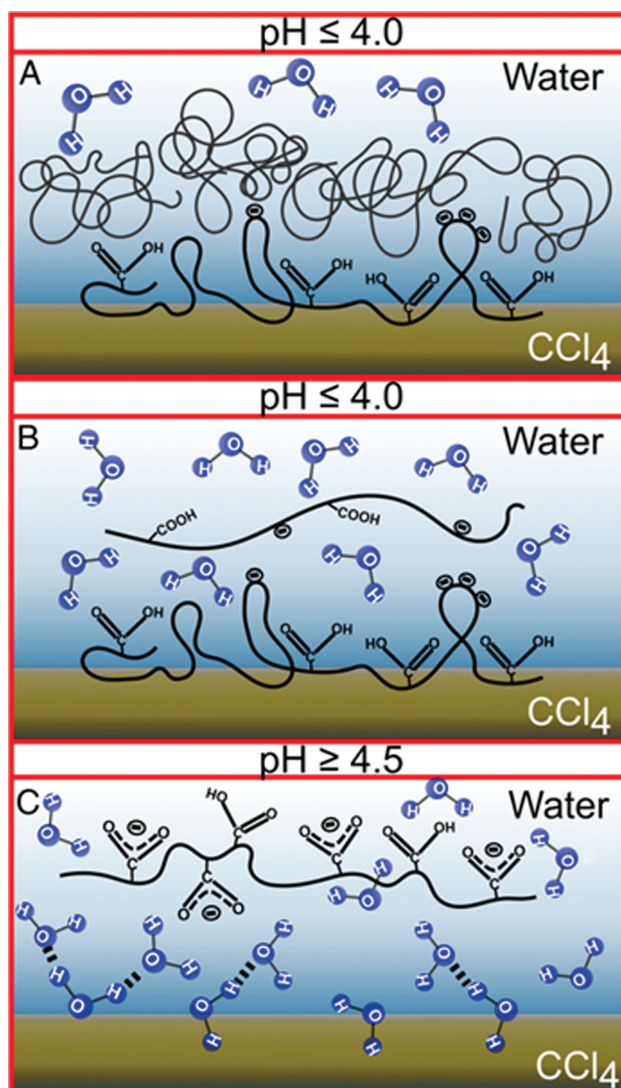


FIGURE 15 Cartoon depicting the adsorption and orientation of PAA and PMAA at the CCl_4 /H₂O interface under different pH conditions: (A) adsorption of PAA and atactic PMAA below the critical pH, where randomly coiled polymer continues to adsorb to the subsurface after the initial oriented layer, (B) isotactic PMAA where there is an initial highly oriented layer observed, but the stretched out configuration of isotactic PMAA prevents continued adsorption to the subsurface, and (C) the lack of interfacial polymer adsorption and the neat CCl_4 /H₂O interface. Reproduced from Ref. 23, copyright PNAS (permission request not required for noncommercial use).

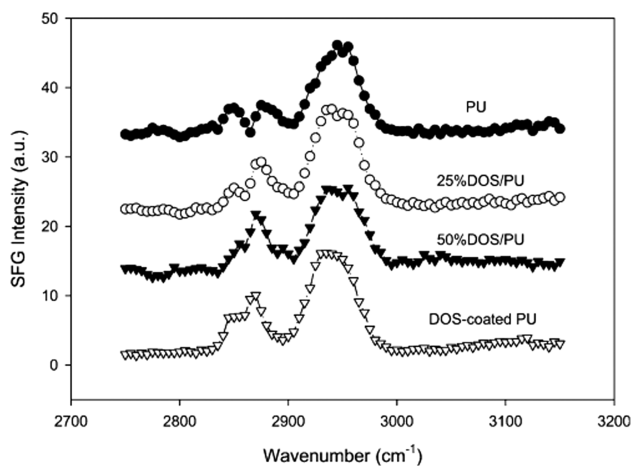


FIGURE 16 SFG spectra of PU, DOS/PU blends, and DOS-coated PU in water. Reproduced from Ref. 25, with permission from the American Chemical Society.

plasticizers may migrate or order themselves at water, effectively covering the polymer. The Chen laboratory published a study on the SFG spectrum of PU in water compared with PU plasticized with dioctyl sebacate, or DOS.²⁵ Figure 16 shows the spectra of PU, PU with 25% DOS, 50% DOS, and PU coated with DOS in water.

The peak assignments for PU were CH_2 (s) at 2850 cm^{-1} , CH_2 (as) at 2920 cm^{-1} , and Fermi resonance at 2945 cm^{-1} . DOS contained CH_3 (s) stretches at 2880 cm^{-1} , CH_2 (s) at 2850 cm^{-1} , and Fermi resonance at 2950 cm^{-1} . The water spectra of PU and plasticized PU were much different from the air interface. The water interface spectrum for DOS-coated PU was similar to the spectrum of PU plasticized with 25 and 50% DOS which suggested the surface of the 25 and 50% DOS/PU films were covered with DOS at that interface. The methyl groups of DOS were present in all three DOS/PU mixtures at the water interface as well. Any spectral changes at the water interface returned to normal on re-exposure to air, suggesting any molecular rearrangement on the surface was reversible.²⁵

As demonstrated in the previous study, molecular behaviors of polymers at the water interface can be greatly influenced by plasticizers within the system. Such behavioral changes are expected as much of molecular movement in water is dominated by a drive to reduce free energy of the system. A second polymer/plasticizer investigation is currently taking place in the Chen laboratory, focusing on plasticized poly(vinyl chloride) (PVC) in water. Small plasticizing molecules are believed to space out long PVC chains and increase free volume of the chain network. As plasticizer molecules have a large effect on bulk PVC, logic follows they would have some degree of influence at a molecular interface. Preliminary results for the polymer/water interface of a system containing PVC plasticized with bis-2-ethylhexyl phthalate demonstrate the methylene groups of PVC order much differently in water depending on the concentration of the plasticizer.

Relationships between Heat, Polymer Orientation, and Wettability

The microscopic ordering behaviors that have been discussed in this article are often responsible for macroscopic properties of polymeric materials. The hydrophobicity or hydrophilicity of a polymer surface, for example, is highly dependent on the concentration and orientation of hydrophobic or hydrophilic functional groups at the air interface.¹⁰ Some polymers exhibit large hysteresis on contact with water, and this behavior may be explained by microscopic surface heterogeneity. The Dhinojwala laboratory wanted to find out why the wettability of poly(vinyl *n*-octadecyl carbamate-*co*-vinyl acetate) increased dramatically with increasing temperatures.⁹⁸ By probing this polymer in water using SFG at different temperatures, they discovered that the microscopic surface energies of the film were quite different due to heating. Shown in Figure 17 is polymer/water interface SFG spectra obtained at different temperatures. Interpreted from this set of spectra is an order to disorder transition temperature range. With increasing temperature the 2873 cm^{-1} peak, assigned to the CH_3 (s) stretch, decreases in intensity. By $81\text{ }^\circ\text{C}$, this peak was not resolvable. However, the intensity of the CH_2 (s) peaks at 2853 and 2860 cm^{-1} remained similar. Because the peak intensity transitions were gradual,

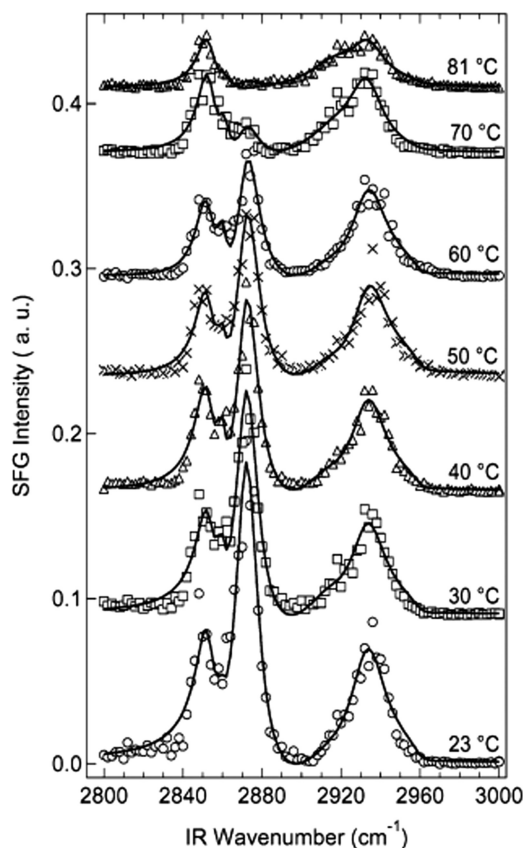


FIGURE 17 Temperature series SFG spectra of the PVNODC/water interface in ssp. The solid lines represent spectral fitting. Reproduced from Ref. 98, with permission from the American Chemical Society.

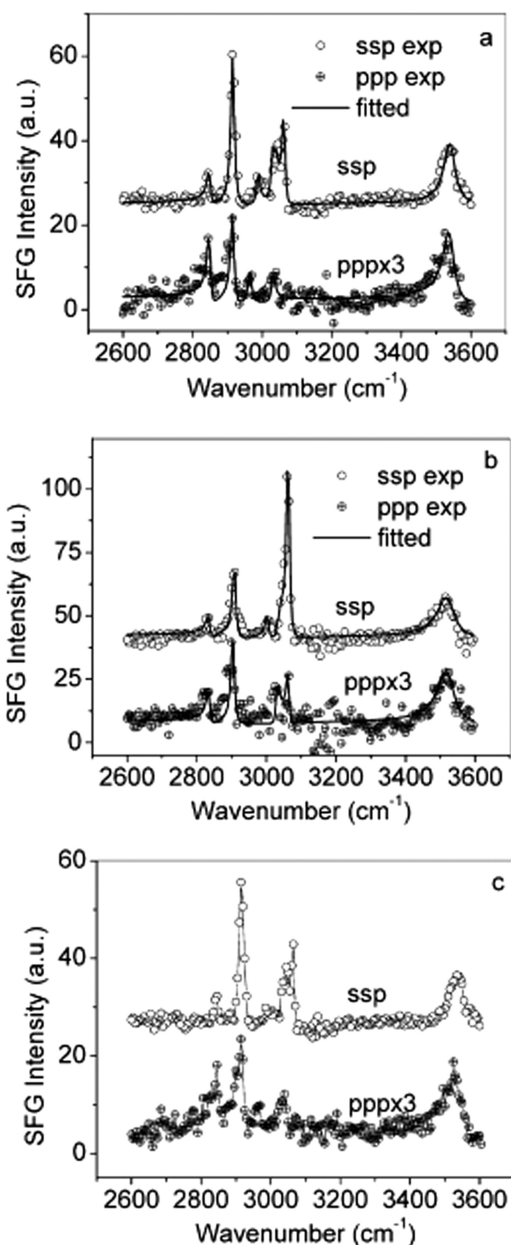


FIGURE 18 The ssp and ppp spectra of BPP surface: (a) annealed at 90 °C for 1 h, (b) annealed at 90 °C for 1 h and then exposed to air for 1 h, (c) annealed at 90 °C for 1 h, then exposed to air for 1 h, and reannealed at 90 °C for 1 h. Reproduced from Ref. 100, with permission from the American Chemical Society.

this suggested a sharp phase transition did not occur at the surface of the film. Calculated theoretical orientation changes of the functional groups could lead to increased wettability, as it was believed the hydrophobic groups lay closer to the polymer bulk with increasing temperature. By coupling the SFG results with contact angle at different temperatures, the Dhinojwala laboratory built a strong case for the microscopic reasoning behind hydrophobicity changes of a polymer film.⁹⁸

Polymers with Phenyl Rings in Water

Many of the articles examined in this review have focused on the microscopic behaviors of methyl and methylene functional groups in water. Numerous industrial polymers contain these small functional groups, but some also contain rigid ring groups. These groups can move independently from a backbone (depending on the stereochemistry of the structure) and preferentially orient themselves at a water interface.⁹⁹

The Richter laboratory used SFG to observe differences in phenyl ring orientation from deuterated polystyrene (d-PS) in low and high surface tension liquids in 2004.²⁷ There are several vibrational modes observable for phenyl rings using SFG, which may red shift in liquid. In water, there are three phenyl ring modes for d-PS at 2289, 2275, and 2261 cm^{-1} , the first and last of which are red-shifted by about 6 wavenumbers from what is observed at the air interface. The Richter laboratory obtained d-PS ssp and sps spectra at air, hexane, and water. Appearing as a negative peak (right side of peak a dip in the background), the phenyl ring intensity in water was much lower in water than air or hexane, which had similar spectra. The negative sign of the vibrational resonance compared to the background showed that the phenyl rings were oriented away from the bulk and toward the interface. The lower intensity of the phenyl vibrations in water suggested the rings were lying down more than in air or hexane. Indeed, when the spectra from ssp and sps polarization combinations were used to calculate the molecular orientation of the interfacial phenyl rings to the surface normal, assuming a delta function, the phenyl rings lay about $35 \pm 4^\circ$ in air, $42 \pm 4^\circ$ in hexane, and $70 \pm 8^\circ$ in water. This article demonstrated that the orientational behavior of much larger polymeric organic groups than methyl groups could be understood in air and in water.²⁷

The Chen laboratory studied model phenolic resins used in microelectronics that fail from increased water content in an effort to better understand phenol orientation changes from humidity content in air.¹⁰⁰ A biphenyl type phenol (BPP) resin was annealed and SFG spectra were obtained in air. The resin was then exposed to 40% RH for 1 h and SFG spectra were taken again. Finally, the resin was reannealed. The resulting spectra can be seen in Figure 18.

The aromatic CH stretches of the phenyl rings were assigned to 3000 and 3060 cm^{-1} and the vibrations from hydroxyl phenol groups were believed to be located at 3540 cm^{-1} . After humidity exposure, the peak at 3063 cm^{-1} increased in intensity. As this peak was assigned to the CH symmetric phenyl stretching, this suggested either that the phenyl ring now stood more perpendicular to the surface or that the phenyl rings across the film surface were more ordered. The 3540 cm^{-1} hydroxyl peak red shifted to 3520 cm^{-1} , suggesting hydrogen bonding between the water and phenol ring. As observed in Figure 18, these spectral changes were reversible. Heating must have removed hydrogen-bonded water molecules from the film surface and the phenol groups rearranged in air to minimize once again the surface energy. This study demonstrated that even a small amount of water in vapor form could have a large impact on phenyl ring

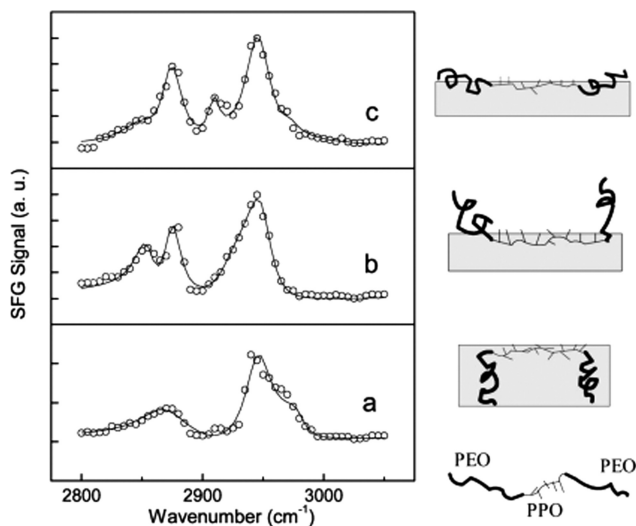


FIGURE 19 SFG spectra (ssp) of the PES/Pluronic F-127 blends with 10 wt % F-127 bulk concentration collected (a) in air, (b) in air immediately after water exposure, and (c) in air after the water treated film was fully dried. Lines represent spectral fitting. Reproduced from Ref. 101, with permission from the American Chemical Society.

behavior in surfaces; the resins in this study needed not be immersed in water to be affected by water molecules.¹⁰⁰ Therefore, it makes sense that phenol-based epoxies may fail or perform differently over time in humid conditions.

Polymers in Air After Water Exposure

We have observed how polymers may be probed at the film/air interface but the effects of water on film structure can still be distinguished. Such studies may apply to biocompatible polymers, which can be immersed in water, removed, and dried many times. Poly(ethersulfone) (PES) may be blended with Pluronic F-127 to increase its biocompatibility. To understand what happens to this blend in air after water immersion, the Chen laboratory took ssp spectra of PES in air, immediately after 1 h of water exposure, and again after the film was fully dried (Fig. 19).¹⁰¹

After water exposure, a peak at 2860 cm^{-1} appeared, assigned to $\text{CH}_2(\text{s})$ of the PEG component within Pluronic F-127. Once dried, this peak was barely resolvable and a signal at 2920 cm^{-1} , which was assigned to $\text{CH}_2(\text{as})$ of PEG increased in intensity. This suggested that the CH_2 groups changed orientation from water contact. Peaks at 2945 and 2875 cm^{-1} were assigned to the CH_3 Fermi resonance and $\text{CH}_3(\text{s})$ vibrations of PPG in Pluronic F-127, respectively. When assuming a Gaussian distribution, the CH_3 groups on the surface of the films were calculated to lie down more and also possibly had a narrower distribution of angles on the surface after water immersion. Unlike the phenyl groups discussed in the previous section, the molecular ordering changes due to water contact were irreversible.

SFG studies on a few more groups of polymers (polymers with plasticizers, polymers with phenyl groups, and so forth) were briefly explored in this section. Here, we have seen that using

SFG, we can observe plasticizer molecules covering a polymer surface in water. In addition, we know polymer behavior may be changed with small amounts of plasticizer present at the water interface. This section also revealed SFG may be used to study large functional groups like phenyl in water. These groups were found to follow similar behavioral trends to small hydrophobic CH groups but also have more movement constraints due to their bulky stereochemistry. After spending the bulk of the review focusing on polymeric behavior in water, we briefly looked at a study of irreversible molecular changes from water contact where CH groups on PES changed orientation after water exposure.

SUMMARY

SFG can be used to derive molecular level behaviors of polymers in a variety of environments *in situ*, including water. It has been shown that much of polymer behavior in water is dominated by a drive to lower the free energy of the system. This may be achieved through hydrogen bonding, hydrophobic/hydrophilic interactions, stereochemistry, or a combination thereof. Such underlying principles were found to be applicable to poly(methylacrylate)s, poly(dimethyl siloxane)s, PEGs, poly(electrolyte)s, and a handful of other polymer types.

We have seen in this review that SFG studies at polymer/water interfaces have granted the scientific community a much better understanding of microscopic functional group behavior in aqueous environments for polymers used in medical, industrial, and marine biofouling applications. Such microscopic trends can be traced to the origins of important macroscopic physical surface properties, furthering the scientific polymer research field. This ultimately increases our ability to understand commonly used polymer behavior with water and allows us to produce better and more technologically advanced polymers and plastics.

ACKNOWLEDGMENTS

The authors thank the support from the National Science Foundation (CHE 1111000), Office of Naval Research (N00014-12-1-0452), and Semiconductor Research Corporation (P13696).

REFERENCES AND NOTES

- 1 H. Y. Erbil, A. L. Demirel, Y. Avci, O. Mert, *Science* **2003**, 299, 1377–1380.
- 2 E. Sackmann, *Science* **1996**, 271, 43–48.
- 3 W. A. Braunecker, K. Matyjaszewski, *Prog. Polym. Sci.* **2007**, 32, 93–146.
- 4 D. Zhang, D. Gracias, R. Ward, M. Gauckler, Y. Tian, Y. Shen, G. Somorjai, *J. Phys. Chem. B* **1998**, 102, 6225–6230.
- 5 G. Riess, *Prog. Polym. Sci.*, **2003**, 28, 1107–1170.
- 6 Z. Chen, Y. Shen, G. A. Somorjai, *Annu. Rev. Phys. Chem.* **2002**, 53, 437–465.
- 7 J. Wang, Z. Paszti, M. A. Even, Z. Chen, *J. Am. Chem. Soc.* **2002**, 124, 7016–7023.
- 8 Z. Hu, Y. Chen, C. Wang, Y. Zheng, Y. Li, *Nature* **1998**, 393, 149–152.

- 9 Z. Ping, Q. Nguyen, S. Chen, J. Zhou, Y. Ding, *Polymer* **2001**, *42*, 8461–8467.
- 10 Z. Chen, *Polym. Int.* **2007**, *56*, 577–587.
- 11 R. Yoshida, K. Uchida, Y. Kaneko, K. Sakai, A. Kikuchi, Y. Sakurai, T. Okano, *Nature* **1995**, *374*, 240–242.
- 12 J. Wen, G. Somorjai, F. Lim, R. Ward, *Macromolecules* **1997**, *30*, 7206–7213.
- 13 L. Feng, S. Li, Y. Li, H. Li, L. Zhang, J. Zhai, Y. Song, B. Liu, L. Jiang, D. Zhu, *Adv. Mater.* **2002**, *14*, 1857–1860.
- 14 K. Ishihara, H. Nomura, T. Mihara, K. Kurita, Y. Iwasaki, N. Nakabayashi, *J. Biomed. Mater. Res.* **1998**, *39*, 323–330.
- 15 H. Otsuka, Y. Nagasaki, K. Kataoka, *Adv. Drug Deliv. Rev.* **2012**, *55*, 403–419.
- 16 S. Krishnan, R. Ayothi, A. Hexemer, J. A. Finlay, K. E. Sohn, R. Perry, C. K. Ober, E. J. Kramer, M. E. Callow, J. A. Callow, *Langmuir* **2006**, *22*, 5075–5086.
- 17 S. Krishnan, C. J. Weinman, C. K. Ober, *J. Mater. Chem.* **2008**, *18*, 3405–3413.
- 18 A. Statz, J. Finlay, J. Dalsin, M. Callow, J. A. Callow, P. B. Messersmith, *Biofouling* **2006**, *22*, 391–399.
- 19 C. B. Kristalyn, X. Lu, C. J. Weinman, C. K. Ober, E. J. Kramer, Z. Chen, *Langmuir* **2010**, *26*, 11337–11343.
- 20 S. Ye, A. McClelland, P. Majumdar, S. J. Stafslie, J. Daniels, B. Chisholm, Z. Chen, *Langmuir* **2008**, *24*, 9686–9694.
- 21 S. Ye, P. Majumdar, B. Chisholm, S. Stafslie, Z. Chen, *Langmuir* **2010**, *26*, 16455–16462.
- 22 D. K. Beaman, E. J. Robertson, G. L. Richmond, *Langmuir* **2011**, *27*, 2104–2106.
- 23 D. K. Beaman, E. J. Robertson, G. L. Richmond, *Proc. Natl. Acad. Sci.* **2012**, *109*, 3226–3231.
- 24 C. Cooper, P. Dubin, A. Kayitmazer, S. Turksen, *Curr. Opin. Colloid Interface Sci.* **2005**, *10*, 52–78.
- 25 M. L. Clarke, J. Wang, Z. Chen, *Anal. Chem.* **2003**, *75*, 3275–3280.
- 26 C. Chen, J. Wang, Z. Chen, *Langmuir* **2004**, *20*, 10186–10193.
- 27 C. S. C. Yang, P. T. Wilson, L. J. Richter, *Macromolecules* **2004**, *37*, 7742–7746.
- 28 S. A. Sukhishvili, S. Granick, *Macromolecules* **2002**, *35*, 301–310.
- 29 M. Krzak, Z. Tabor, P. Nowak, P. Warszyński, A. Karatzas, I. A. Kartsonakis, G. C. Kordas, *Prog. Org. Coat.* **2012**, *75*, 207–214.
- 30 D. Li, J. N. Borys, J. M. Lupton, *Appl. Phys. Lett.* **2012**, *100*, 1419071–1419074.
- 31 M. De Jesus, K. Giesfeldt, J. Oran, N. Abu-Hatab, N. Lavrik, M. Sepaniak, *Appl. Spectrosc.* **2005**, *59*, 1501–1508.
- 32 M. Baibarac, M. Lapkowski, A. Pron, S. Lefrant, I. Baltog, *J. Raman Spectrosc.* **1998**, *29*, 825–832.
- 33 W. Chrzanowski, A. Kondyurin, J. H. Lee, M. S. Lord, M. M. M. Bilek, H. W. Kim, *J. Mater. Sci. Mater. Med.* **2012**, *23*, 2203–2215.
- 34 P. G. Rouxhet, M. J. Genet, *Surf. Interface Anal.* **2011**, *43*, 1453–1470.
- 35 W. Chen, T. J. McCarthy, *Macromolecules* **1997**, *30*, 78–86.
- 36 F. Du, R. C. Scogna, W. Zhou, S. Brand, J. E. Fischer, K. I. Winey, *Macromolecules* **2004**, *37*, 9048–9055.
- 37 H. Zhao, X. Liu, N. Fu, Q. Zhang, N. Wang, L. He, X. Qu, *J. Appl. Polym. Sci.* **2012**, *125*, 3419–3428.
- 38 Y. Cho, H. S. Sundaram, J. A. Finlay, M. D. Dimitriou, M. E. Callow, J. A. Callow, E. J. Kramer, C. K. Ober, *Biomacromolecules* **2012**, *13*, 1864–1874.
- 39 M. D. Dimitriou, Z. L. Zhou, H. S. Yoo, K. L. Killups, J. A. Finlay, G. Cone, H. S. Sundaram, N. A. Lynd, K. P. Barteau, L. M. Campos, D. A. Fischer, M. E. Callow, J. A. Callow, C. K. Ober, C. J. Hawker, E. J. Kramer, *Langmuir* **2011**, *27*, 13762–13772.
- 40 H. Ade, A. P. Hitchcock, *Polymer* **2008**, *49*, 643–675.
- 41 Y. R. Shen, *The Principles of Nonlinear Optics*; Wiley-Interscience: New York, **1984**.
- 42 Y. Shen, *Nature* **1989**, *337*, 519–525.
- 43 Z. Chen, *Prog. Polym. Sci.* **2010**, *35*, 1376–1402.
- 44 D. Zhang, R. Ward, Y. Shen, G. Somorjai, *J. Phys. Chem. B* **1997**, *101*, 9060–9064.
- 45 Z. Chen, R. Ward, Y. Tian, S. Baldelli, A. Opdahl, Y. R. Shen, G. A. Somorjai, *J. Am. Chem. Soc.* **2000**, *122*, 10615–10620.
- 46 K. Gautam, A. Schwab, A. Dhinojwala, D. Zhang, S. Dougal, M. Yeganeh, *Phys. Rev. Lett.* **2000**, *85*, 3854–3857.
- 47 J. Wang, C. Chen, S. M. Buck, Z. Chen, *J. Phys. Chem. B* **2001**, *105*, 12118–12125.
- 48 A. Opdahl, T. S. Koffas, E. Amitay-Sadovsky, J. Kim, G. A. Somorjai, *J. Phys.: Condens. Matter* **2004**, *16*, R659.
- 49 A. G. Lambert, P. B. Davies, D. J. Neivandt, *Appl. Spectrosc. Rev.* **2005**, *40*, 103–145.
- 50 T. S. Koffas, E. Amitay-Sadovsky, J. Kim, G. A. Somorjai, *J. Biomater. Sci. Polym. Ed.* **2004**, *15*, 475–509.
- 51 X. Lu, M. L. Clarke, D. Li, X. Wang, G. Xue, Z. Chen, *J. Phys. Chem. C* **2011**, *115*, 13759–13767.
- 52 D. Wu, Y. Guo, G. M. Liu, G. Z. Zhang, *Chin. Sci. Bull.* **2012**, *57*, 984–991.
- 53 M. L. Clarke, C. Chen, J. Wang, Z. Chen, *Langmuir* **2006**, *22*, 8800–8806.
- 54 J. Wang, S. E. Woodcock, S. M. Buck, C. Chen, Z. Chen, *J. Am. Chem. Soc.* **2001**, *123*, 9470–9471.
- 55 D. Zhang, Y. Shen, G. A. Somorjai, *Chem. Phys. Lett.* **1997**, *281*, 394–400.
- 56 J. Kim, A. Opdahl, K. C. Chou, G. A. Somorjai, *Langmuir* **2003**, *19*, 9551–9553.
- 57 R. W. Boyd, *Nonlinear Optics*, 3rd ed.; Burlington, MA: Academic Press, **2008**; Section 3.6, p. 170–179.
- 58 C. Hirose, N. Akamatsu, K. Domen, *Appl. Spectrosc.* **1992**, *46*, 1051–1072.
- 59 X. Zhuang, P. B. Miranda, D. Kim, Y. R. Shen, *Phys. Rev. B* **1999**, *59*, 12632–12640.
- 60 A. J. Moad, G. J. Simpson, *J. Phys. Chem. B* **2004**, *108*, 3548–3562.
- 61 C. Hirose, N. Akamatsu, K. Domen, *J. Chem. Phys.* **1992**, *96*, 1097–1004.
- 62 R. Lu, W. Gan, B. Wu, H. Chen, H. Wang, *J. Phys. Chem. B* **2004**, *108*, 7297–7306.
- 63 H. F. Wang, W. Gan, R. Lu, Y. Rao, B. H. Wu, *Int. Rev. Phys. Chem.* **2005**, *24*, 191–256.
- 64 K. Wolfrum, A. Laubereau, *Chem. Phys. Lett.* **1994**, *228*, 83–88.
- 65 S. Ye, G. Liu, H. Li, F. Chen, X. Wang, *Langmuir* **2012**, *28*, 1374–1380.
- 66 G. Li, S. Ye, S. Morita, T. Nishida, M. Osawa, *J. Am. Chem. Soc.* **2004**, *126*, 12198–12199.
- 67 C. Chen, M. L. Clarke, J. Wang, Z. Chen, *Phys. Chem. Chem. Phys.* **2005**, *7*, 2357–2363.
- 68 A. A. McClelland, Sum Frequency Generation Vibration Spectroscopy Investigation of Buried Polymer and Organic

- Interfaces. Dissertations and Theses (Ph.D. and Master's); University of Michigan Ann Arbor, Ann Arbor MI, USA., **2009**, Chapter 4, pp 66–88.
- 69** A. Mata, A. J. Fleischman, S. Roy, *Biomed. Microdevices* **2005**, *7*, 281–293.
- 70** Q. W. Yuan, J. E. Mark, *Macromol. Chem. Phys.* **1999**, *200*, 206–220.
- 71** S. Hu, X. Ren, M. Bachman, C. E. Sims, G. Li, N. Allbritton, *Anal. Chem.* **2002**, *74*, 4117–4123.
- 72** J. H. Park, K. D. Park, Y. H. Bae, *Biomaterials* **1999**, *20*, 943–954.
- 73** S. Lee, J. Vörös, *Langmuir* **2005**, *21*, 11957–11962.
- 74** I. Wong, C. M. Ho, *Microfluid Nanofluid.* **2009**, *7*, 391–306.
- 75** Q. Shi, S. Ye, S. A. Spanninga, Y. Su, Z. Jiang, Z. Chen, *Soft Matter* **2009**, *5*, 3487–3494.
- 76** E. Hsiao, A. L. Barnette, L. C. Bradley, S. H. Kim, *ACS App. Mater. Interface* **2011**, *3*, 4236–4241.
- 77** C. Kim, M. C. Gurau, P. S. Cremer, H. Yu, *Langmuir* **2008**, *24*, 10155–10160.
- 78** Z. Wu, W. Tong, W. Jiang, X. Liu, Y. Wang, H. Chen, *Colloids Surf. B* **2012**, *96*, 37–43.
- 79** Y. H. Choi, J. C. Kim, J. K. Ahn, S. Y. Ko, D. H. Kim, T. Lee, *J. Ind. Eng. Chem.* **2008**, *14*, 292–296.
- 80** J. Tiller, C. Sprich, L. Hartmann, *J. Controlled Release* **2005**, *103*, 355–367.
- 81** R. R. Pant, P. A. Fulmer, M. B. Harney, J. P. Buckley, J. H. Wynne, *J. Appl. Polym. Sci.* **2009**, *113*, 2397–2403.
- 82** T. Kondo, K. Nomura, M. Murou, M. Gemmei-Ide, H. Kitano, H. Noguchi, K. Uosaki, K. Ohno, Y. Saruwatari, *Colloids Surf. B* **2012**, *100*, 126–132.
- 83** L. Zhang, A. Eisenberg, *Science* **1995**, *268*, 1728–1731.
- 84** A. S. De León, A. Del Campo, M. Fernández-García, J. Rodríguez-Hernández, A. Muñoz-Bonilla, *Langmuir* **2012**, *28*, 9778–9787.
- 85** A. Stocco, K. Tauer, S. Pispas, R. Sigel, *J. Colloid Interface Sci.* **2011**, *355*, 172–178.
- 86** N. Reitzel, D. R. Greve, K. Kjaer, P. B. Howes, M. Jayaraman, S. Savoy, R. D. McCullough, J. T. Mcdevitt, T. Bjornholm, *J. Am. Chem. Soc.* **2000**, *122*, 5788–5800.
- 87** R. Sedev, G. Findenegg, D. Exerowa, *Colloid. Polym. Sci.* **2000**, *278*, 119–123.
- 88** C. Chen, M. A. Even, Z. Chen, *Macromolecules* **2003**, *36*, 4478–4484.
- 89** O. N. Tretinnikov, *J. Adhes. Sci. Technol.* **1999**, *13*, 1085–1102.
- 90** C. Chen, M. A. Even, J. Wang, Z. Chen, *Macromolecules* **2002**, *35*, 9130–9135.
- 91** M. A. Even, C. Chen, J. Wang, Z. Chen, *Macromolecules* **2006**, *39*, 9396–9401.
- 92** L. Dreesen, C. Humbert, P. Hollander, A. Mani, K. Ataka, P. Thiry, A. Peremans, *Chem. Phys. Lett.* **2001**, *333*, 327–331.
- 93** M. T. L. Casford, P. B. Davies, D. J. Neivandt, *Langmuir* **2006**, *22*, 3105–3111.
- 94** M. T. L. Casford, P. B. Davies, D. J. Neivandt, *Langmuir* **2003**, *19*, 7386–7391.
- 95** R. Windsor, D. J. Neivandt, P. B. Davies, *Langmuir* **2002**, *18*, 2199–2204.
- 96** S. Ye, S. Nihonyanagi, K. Uosaki, *Phys. Chem. Chem. Phys.* **2001**, *3*, 3463–3469.
- 97** X. Chen, J. Wang, C. B. Kristalyn, Z. Chen, *Biophys. J.* **2007**, *93*, 833–875.
- 98** H. Rangwalla, A. D. Schwab, B. Yurdumakan, D. G. Yablon, M. S. Yeganeh, A. Dhinojwala, *Langmuir* **2004**, *20*, 8625–8633.
- 99** V. Marcon, D. Fritz, N. F. A. Van Der Vegt, *Soft Matter* **2012**, *8*, 5585–5594.
- 100** X. Lu, J. Han, N. Shephard, S. Rhodes, A. D. Martin, D. Li, G. Xue, Z. Chen, *J. Phys. Chem. B* **2009**, *113*, 12944–12951.
- 101** Q. Shi, S. Ye, C. Kristalyn, Y. Su, Z. Jiang, Z. Chen, *Langmuir* **2008**, *24*, 7939–7946.